

MODELLING OF THE TURBULENT WALL JET GENERATED BY A PITCHED BLADE TURBINE IMPELLER. THE EFFECT OF TURBULENCE MODEL

Zdzislaw Jaworski* and Barbara Zakrzewska

Chemical Engineering Faculty, Technical University of Szczecin, Szczecin, Poland

*also School of Engineering, The University of Birmingham, Birmingham

CFD modelling results have been presented for a flat-bottomed tank with a pitched blade turbine impeller and four baffles. Four turbulence models, i.e. the standard k- ϵ , the RNG k- ϵ , the realizable k- ϵ and the Reynolds stress model have been used in the modelling. The simulated values of the tangential and axial mean velocity components along with the kinetic energy of turbulence have been compared for the wall jet region with the corresponding experimental data from LDA. The best results have been obtained for the standard k- ϵ model with a good accuracy for the mean velocity and a significant underprediction of the turbulent kinetic energy.

Keywords: CFD, flow modelling, wall jet, pitched blade turbine

INTRODUCTION

The numerical modelling of transport processes in stirred tanks with a pitched blade turbine impeller has been widely accomplished by application of Computational Fluid Dynamics (CFD) codes, in spite of the flow complexity and resulting difficulties in the modelling¹⁻⁴. In particular, this relates to the region adjacent to the tank walls, called the wall jet, where usually wall functions have been used for the turbulent flow modelling.

Struesson et al.⁵ investigated the turbulent flow behaviour in the vicinity of the tank wall and bottom. They applied the low Reynolds number, k- ϵ model of turbulence along with the wall functions. However, it was not a fully predictive modelling since the boundary conditions at the impeller region surface were defined by means of the mean velocity components and the kinetic turbulence energy obtained from LDA. This resulted in an underprediction of the mean velocity profiles.

In an earlier study⁶ of jacket heat transfer in stirred tanks, it was concluded that the most likely cause of about 1/3 underprediction of the heat transfer coefficient was an imperfect prediction of momentum transfer in the wall jet. This study aims at determining of the effect of the applied turbulence models on the flow modelling results.

MODELLING

The CFD simulation results for a flat-bottomed tank of the diameter, $T = H = 0.202\text{m}$, equipped with four standard baffles and a pitched blade turbine (PBT) impeller is presented in the paper. The applied impeller had a diameter, D , equal to $0.336T$, and it was located axially in the tank with the off-bottom clearance of $C = 0.333H$. LDA experimental data for the mean and fluctuating parts of both the tangential and the axial velocity components in such the geometrical system were presented elsewhere⁷. The PBT impeller rotated with the speed of $N = 290$ rpm, which resulted in Reynolds number, $Re = 22500$. Those measurements were carried out in the vicinity of the tank wall at 154 points, which were defined by a grid of 14 axial (z/H from 0.09 to 0.83) and 11 radial ($y = 1, 2, 4, 6, 8, 10, 12, 14, 16, 18, 20$ mm) positions. The experimental data⁷ were used for validating of the CFD predictions obtained in this study.

The turbulent momentum transfer simulations for the stirred tank were performed with the help of the commercial CFD code, FluentTM 5.4. In the computations, the standard

Reynolds averaged Navier-Stokes (RANS) equations for the differential mass and momentum balance were numerically solved, c.f. Eq. (1) for the generalized variable \mathbf{f} .

$$\frac{\partial(\mathbf{r}\mathbf{f})}{\partial t} + \frac{\partial}{\partial x_i}(\mathbf{r}u_i\mathbf{f}) - \frac{\partial}{\partial x_i} \left(\mathbf{G}_{eff} \frac{\partial \mathbf{f}}{\partial x_i} \right) - S_f = 0 \quad (1)$$

In order to close the set of the four differential equations, different turbulence models were employed. Three of them stemmed from the two-equation k - ϵ family, i.e. the standard k - ϵ ⁸, RNG k - ϵ ⁹, realizable k - ϵ ¹⁰, and the fourth model was the six-equation Reynolds stress model accompanied also by the \mathbf{e} equation.

The two-equation models consist of one differential transport equation for the turbulent kinetic energy, k Eq. (2), and one for its dissipation rate, \mathbf{e} Eq.(3). The models differ mainly by the definition of the source term in the equation for \mathbf{e} (Table 1) and only slightly by the values of the constants in Eqs. (2, 3)

$$\frac{\partial(\mathbf{r}k)}{\partial t} + \frac{\partial}{\partial x_i}(\mathbf{r}u_i k) = \frac{\partial}{\partial x_i} \left(\mathbf{r} \frac{\mathbf{n}_{eff}}{\mathbf{s}_k} \frac{\partial k}{\partial x_i} \right) + \mathbf{r}(P_k - \mathbf{e}) \quad (2)$$

$$\frac{\partial(\mathbf{r}\mathbf{e})}{\partial t} + \frac{\partial}{\partial x_i}(\mathbf{r}u_i \mathbf{e}) = \frac{\partial}{\partial x_i} \left(\mathbf{r} \frac{\mathbf{n}_{eff}}{\mathbf{s}_e} \frac{\partial \mathbf{e}}{\partial x_i} \right) + S_e \quad (3)$$

The specialised preprocessor MixSimTM 1.7 was used to generating an unstructured numerical grid for the stirred tank with the Multiple Reference Frames (MRF) option. The preprocessor allowed to define the tank geometry, the grid density, physical fluid properties and the boundary conditions. The non-slip conditions were chosen at all fluid-solid boundaries and the symmetry conditions at the free surface of the stirred liquid.

The effect of the numerical grid density on the CFD simulated flow in the wall jet region was reported elsewhere¹¹. It was concluded that the CFD results were closest to the LDA data when the initial grid density of 40 cells per tank diameter was used prior to grid adaption. The same grid density and adaption method were applied in this study.

The first step in the momentum transfer simulations was computing an approximate (pseudo-laminar) velocity field obtained without activating a turbulence model and for the initial grid. In the next step, one of the four turbulence models and the standard wall functions were employed in the simulations of the turbulent momentum transfer in the stirred tank. Those computations were carried out till the normalised sum of residuals fell below 10^{-7} . Then, the logarithmic wall function recommendations for the cells adjacent to the solid boundaries were taken into account for the grid adaption (refinement). The recommendations require the dimensionless off-wall distance value, y^+ , of the cell centre to be within the range from 30 to 60. Those grid cells, which did not fulfil the criterion were automatically divided to conform with the recommendations. This happened to 235 cells, only at the impeller blades, and resulted in 705 new cells. The total cell number of the refined grid was 112601. The final grid of the stirred tank in the mid-plane between two baffles is visualized in Fig.1. With the refined grid, the simulations were re-run to fulfil the convergence criterion of the residual sum lower than 10^{-7} .

In the next stage, the tangential and axial components of liquid velocity and also the kinetic energy of turbulence, which were computed for each of the four turbulence models, were compared with the experimental data from LDA⁷. The LDA values of the kinetic energy of turbulence, k_{LDA} , were computed from Eq. (4) where it was assumed that the third component of the energy is equal to the mean value of the two components measured.

$$k_{LDA} = \frac{1.5}{2} (u_t'^2 + u_z'^2) \quad (4)$$

Based on that comparison, it was assessed which of the four tested turbulence models described most accurately the investigated velocity field in the tank stirred by the pitched blade turbine impeller.

MODELLING RESULTS

The CFD simulated values of the axial, u_z , and tangential, u_t , mean velocity components and the kinetic energy of turbulence, k , obtained for the four turbulence tested, were plotted together with their counterparts from LDA measurements in form of axial profiles along the tank wall. The velocities were standardized (U_z , U_t) by dividing them by the impeller tip velocity, pDN . The total number of analysed profiles was $11 \times 3 = 33$ and examples of such the profiles are shown in Figs. 2, 3 and 4 for the axial and tangential velocity components and the kinetic turbulence energy, respectively. Graphs for only 3 of 11 radial distances, y , were shown in the figures.

AXIAL VELOCITY

The axial profiles of the dimensionless axial velocity, U_z , obtained both from LDA and CFD were qualitatively very similar for all tested radial distances off the tank wall, c.f. Fig.2. With the increasing distance from the wall, the profiles became flatter. The maximum U_z values were obtained at the closest location to the wall, i.e. at the radial distance of $y = 1$ mm, both in the experiments⁷ and simulations. It should be mentioned that close to the free surface and at the radial distances of y , from 1 to 4 and 8 mm the experimental axial mean velocities, u_z , were slightly positive (upward, induced flow) whereas the simulated equivalents were always negative, irrespective of the turbulence model employed.

The closest agreement between the modelling predictions and experiments for the axial mean velocity was achieved for the standard k- ϵ turbulence model and the widest discrepancy was concluded for the realizable k- ϵ . The mean deviation of the axial normalized velocities from the LDA and CFD data sets was computed for all 154 axial and radial points and it was 2.2; 5.2; 3.9 and 3.9% for the standard k- ϵ , the realizable, the RNG and the RSM model, respectively. However, in the lower half of the stirred tank ($z/H = 0.09$ to 0.53) the deviation was smaller, i.e. 1.6; 4.0; 3.1 and 2.8%, respectively. The discrepancies were close to the experimental LDA accuracy, which was estimated to be about 1.5% of the impeller tip velocity⁷. Using the proposed criterion¹² for the CFD prediction quality, one can conclude that the ratio of the mean deviation of CFD-LDA results to the LDA measurement accuracy was about 1.4; 3.5; 2.6 and 2.6 for the four turbulence models. These results suggest that the use of the standard k- ϵ model led to high accuracy predictions and the other models except the realizable delivered fair accuracy data.

TANGENTIAL VELOCITY

Examples of axial profiles for the tangential mean velocity component are shown in Fig. 3. Here again, both the LDA and CFD profiles were qualitatively similar. The tangential velocity values simulated with the use of all tested turbulence models were approximately equal at the radial distances from $y = 1$ to 10 mm. The experimental data show small negative (opposite to the impeller rotation) tangential velocities at $z/H = 0.88$, i.e. close to the free surface. None of the turbulence models allowed to predict such negative velocities at the radial distances, y , from 1 to 10 mm. However, further from the tank wall such negative values were predicted in the case of the standard and the RNG k- ϵ models, c.f. Fig. 3.

The CFD predicted mean tangential velocities differed from the corresponding LDA data less than for the axial velocity component and the average differences were 0.90; 0.88; 0.85 and 0.85% of the impeller tip velocity, pDN , for the standard k- ϵ , the realizable, the RNG and the Reynolds stress model, respectively. The discrepancies for each of the turbulence models are within the experimental LDA error of about 1.5% pDN , thus all the models can be regarded as very good in predicting the tangential mean velocities in the stirred tank modelled.

TURBULENCE KINETIC ENERGY

The kinetic turbulence energy values simulated with any of the turbulence models tested were significantly underpredicted in comparison with the k_{LDA} values computed from Eq. (4). The highest deviations were obtained close to the tank wall (for $y = 1$ to 4 mm) and also at the tank bottom. However, the k and k_{LDA} profiles were qualitatively similar. Examples of those profiles for three off-wall distances, y , are depicted in Fig. 4.

The standard k- ϵ model employed in the RANS simulations resulted in the highest values of the volume averaged kinetic turbulence energy, k_{ave} , of $0.0020 \text{ m}^2/\text{s}^2$. The corresponding k values for the realizable k- ϵ , the RNG k- ϵ and the Reynolds stress model were 0.0011 ; 0.0013 and $0.0014 \text{ m}^2/\text{s}^2$, respectively. Fig. 5 visualises the distribution of the simulated k values in the mid-plane between two neighbouring baffles for the four turbulence models applied.

The average (resultant) fluctuating velocity values, u'_{res} and u' , were estimated respectively from the k_{LDA} and k values, assuming isotropy of turbulence. The differences between the two fluctuating velocities were 5.3; 6.3; 5.8; and 5.5% pDN for the standard k- ϵ , the realizable, the RNG and the Reynolds stress model, respectively. They turned out to be also significantly higher than the corresponding experimental error of about 1.5% pDN . It is interesting that the best approximation was obtained for the standard k- ϵ model in the lower tank half, whereas the RSM delivered best results in the upper half.

There is a general agreement, e.g. papers^{13, 14}, that the standard k- ϵ model used in stirred tanks with both the sliding mesh technique and the multiple reference frames option results in underprediction of the k values in the impeller discharge stream. Application of the RNG k- ϵ or RSM models does not improve the turbulence predictions¹⁴. Thus the kinetic turbulence energy is also underpredicted in the wall jet region, as reported in this study. The authors are of the opinion that the major reason for that originates from the RANS approach, which is by definition unable to evaluate the relatively high contribution of the flow macro-instabilities in turbulently stirred tanks. On the other hand, the experimental turbulence energy can be largely overestimated¹⁴, if the impeller blade passage effect is not filtered out.

CONCLUDING REMARKS

The study aimed at establishing the turbulence model effect on the quality of the CFD predictions. Modelling of the turbulent momentum transfer in the stirred tank was carried out with the use of the standard wall functions and four different turbulence models, i.e. the standard k- ϵ , RNG k- ϵ , the realizable k- ϵ and the Reynolds stress model. The simulation results were compared with LDA experimental data⁷ for the wall jet region in the tank and the following conclusions were drawn from the analysis of the modelling results:

1. The axial mean velocity component was predicted well with the help of the standard k- ϵ turbulence model. The other models led to less accurate simulation results.
2. The tangential mean velocity values were simulated with a very good accuracy, irrespective of the turbulence model.

3. The kinetic energy of turbulence was underpredicted in the modelling for all the turbulence models, however, the standard k- ϵ model delivered the smallest deviations from experiments.

NOMENCLATURE

C	impeller off-bottom clearance, m
C_m, C_1, C_2	constants in turbulence models
D	impeller diameter, m
H	liquid level in the tank, m
k	turbulence kinetic energy, m^2/s^2
k_{ave}	volume averaged kinetic turbulence energy, m^2/s^2
N	impeller rotational speed, 1/s
P_k	production of turbulence kinetic energy, m^2/s^3
r	radial coordinate, m
Re	Reynolds number
$S_{i,j}$	mean strain rate, 1/s
S	source term
T	tank diameter, m
t	time, s
u'_z, u'_t	axial and tangential fluctuating velocity components, m/s
u_z, u_t	axial and tangential mean velocity components, m/s
U_z, U_t	non-dimensional axial and tangential mean velocity components
x_i	Cartesian coordinate, m
y	radial distance from tank wall, m
z	axial coordinate, m

Greek letters

ρ	density, kg/m^3
ϵ	dissipation rate of turbulence kinetic energy, m^2/s^3
f	generalized variable
ν, ν_t, ν_{eff}	laminar, turbulent and effective kinematic viscosity, m^2/s
G_{eff}	effective diffusivity
S_k, S_ϵ	turbulent Prandtl numbers for k and ϵ

REFERENCES

1. Bakker A., Myers K.J., Ward R.W., Lee C.K., 1996, The laminar and turbulent flow pattern of a pitched blade turbine, *Trans IChemE*, **74**: 485-491.
2. Armenante P.M., Chou C.C., 1996, Velocity profiles in a baffled vessel with single or double pitched-blade turbines, *AIChE J.*, **42** (1): 42-54.
3. Sahu A.K., Kumar P., Joshi J.B., 1998, Simulation of flow in stirred vessel with axial flow impeller: zonal modelling and optimization of parameters, *Ind. Eng. Chem. Res.*, **37**: 2116-2130.
4. Jaworski Z., Dyster K.N., Nienow A.W., 2001, The effect of size, location and pumping direction of pitched blade turbine impellers on flow patterns: LDA measurements and CFD predictions, *Trans IChemE*, **79**: 887-894.
5. Struesson C., Theliander H., Rasmuson A., 1995, An experimental (LDA) and numerical study of the turbulent flow behavior in the near wall and bottom regions in an axially stirred vessel, *AIChE Symp. Ser.*, 91 (305): 102-114.

6. Jaworski Z., 27-31.08.2000, Numerical studies on jacket heat transfer in stirred tanks, *CHISA 2000 Congress, Prague*, paper G7.1.
7. Zakrzewska B., Peryt S., Jaworski Z., 2001, A study of transitional and turbulent boundary flows in a stirred tank. I. LDA measurements, *Inż. Chem. Proc.*, **22**: 427-443.
8. Launder B. E., Spalding D. B., 1974, The numerical computation of turbulent flows, *Comp. Meth. in App. Mech. and Eng.*, **3**: 269-289.
9. Orszag S.A., Yakhot V., 1994, Recent ideas on turbulence transport modeling, *2nd World Conference in Applied CFD*, pp.8.1 – 8.7.
10. Shih T.-H., Liou W.W., Shabbir A., Zhu J., 1995, A new k- ϵ eddy-viscosity model for high Reynolds number turbulent flows – model development and validation, *Computers fluids*, **24** (3): 227-238.
11. Zakrzewska B., Jaworski Z., 2002, Modelling of the turbulent wall jet generated by a pitched blade turbine impeller. The effect of grid density, *9th Polish Seminar "Mixing"*, Olsztyn, Poland, 18 – 20 Sept. 2002, accepted.
12. Jaworski Z., Wyszynski M.L., Moore I.P.T., Nienow A.W., 1997, Sliding mesh computational fluid dynamics – a predictive tool in stirred tank design, *Proc Instn Mech Engrs*, **211 A**: 149-156.
13. Lane G.L., Schwarz M.P., Evans G.M., 2000, Comparison of CFD methods for modelling of stirred tanks, *10th European Conference on Mixing, Delft, The Netherlands*, 273-280.
14. Syrjänen J.K., Manninen M.T., 2000, Detailed CFD prediction of flow around a 45° pitched blade turbine, *10th European Conference on Mixing, Delft, The Netherlands*, 265-272.

ACKNOWLEDGEMENTS

The authors gratefully acknowledge financial support from the State Committee for Scientific Research in Poland and the kind donation of the MixSim™ software by Fluent Europe.

ADDRESS

Correspondence concerning this paper should be addressed to Z. Jaworski, Technical University of Szczecin, Chemical Engineering Department, Al. Piastow 42, 71-065 Szczecin, Poland.

E-mail: z.jaworski@bham.ac.uk

turbulence model	S_e and model constants
standard k- ϵ ⁸	$\mathbf{r} \left(C_{1,S} \frac{\mathbf{e}}{k} P_k - C_{2,S} \frac{\mathbf{e}}{k} \mathbf{e} \right)$ $C_m = 0.09; C_{1,S} = 1.44; C_{2,S} = 1.92; \mathbf{s}_{k,S} = 1; \mathbf{s}_{e,S} = 1.314$
RNG k- ϵ ⁹	$\mathbf{r} \left(C_{1,RNG} \frac{\mathbf{e}}{k} P_k - \mathbf{a} \frac{\mathbf{e}}{k} \mathbf{e} - C_{2,RNG} \frac{\mathbf{e}}{k} \mathbf{e} \right) \quad \mathbf{a} = C_m \mathbf{h}^3 \frac{1 - \mathbf{h}/\mathbf{h}_0}{1 + \mathbf{b}\mathbf{h}^3}$ $C_m = 0.0845; C_{1,RNG} = 1.42; C_{2,RNG} = 1.68; \mathbf{s}_{k,RNG} = \mathbf{s}_{e,RNG} = 0.719$
realizable k- ϵ ¹⁰	$\mathbf{r} \left(C_1 S \mathbf{e} - C_2 \frac{\mathbf{e}^2}{k + \sqrt{\mathbf{n}\mathbf{e}}} \right) \quad C_1 = \max \left[0.43, \frac{\mathbf{h}}{\mathbf{h} + 5} \right]$ $C_m = 0.09; C_2 = 1.9; \mathbf{s}_k = 1; \mathbf{s}_e = 1.2$
$P_k = \mathbf{n}_t \left(\frac{\partial u_i}{\partial x_j} + \frac{\partial u_j}{\partial x_i} \right) \frac{\partial u_i}{\partial x_j}$ $\mathbf{h} = S \frac{k}{\mathbf{e}}; \quad S^2 = 2S_{ij}S_{ij}; \quad S_{ij} = 0,5 \left(\frac{\partial u_i}{\partial x_j} + \frac{\partial u_j}{\partial x_i} \right)$	

Table 1. The source terms in the k- ϵ model equations tested
[HYPERLINK](#)

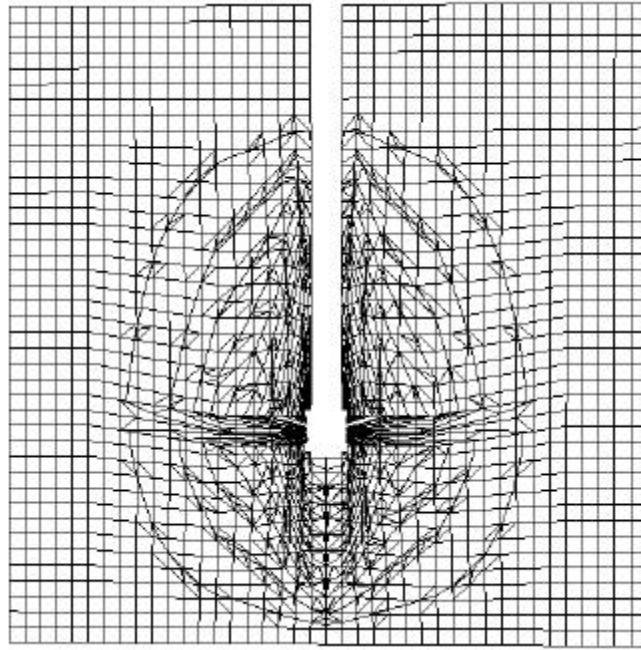


Fig.1. The numerical grid shown in the 45° plane between neighbouring baffles.

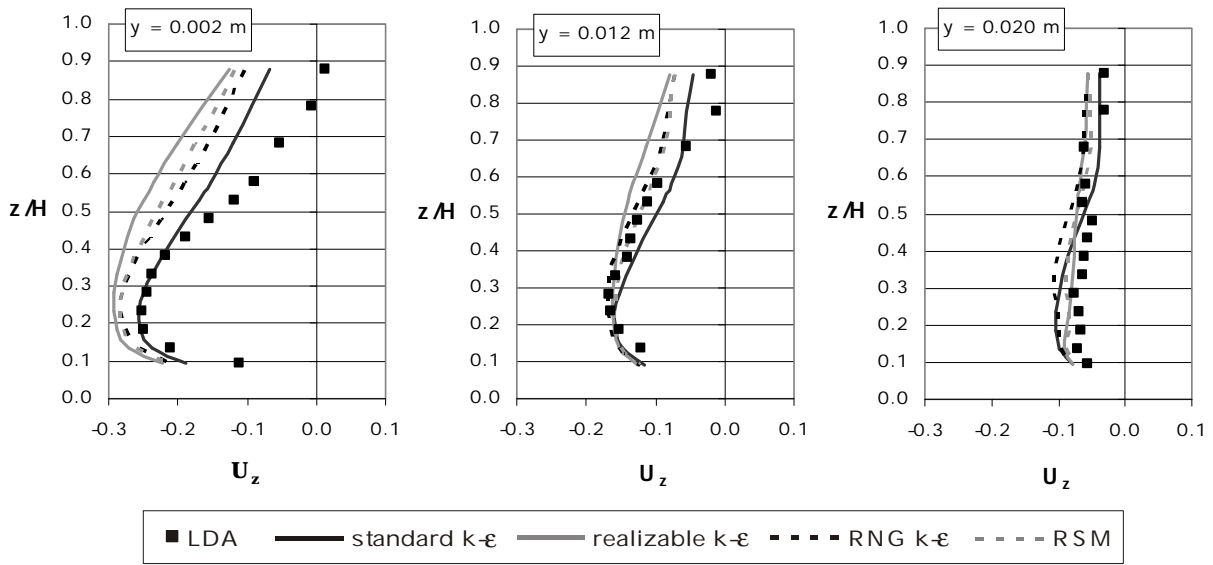


Fig. 2. The axial profiles of the axial mean velocity at three distances from the tank wall, y .

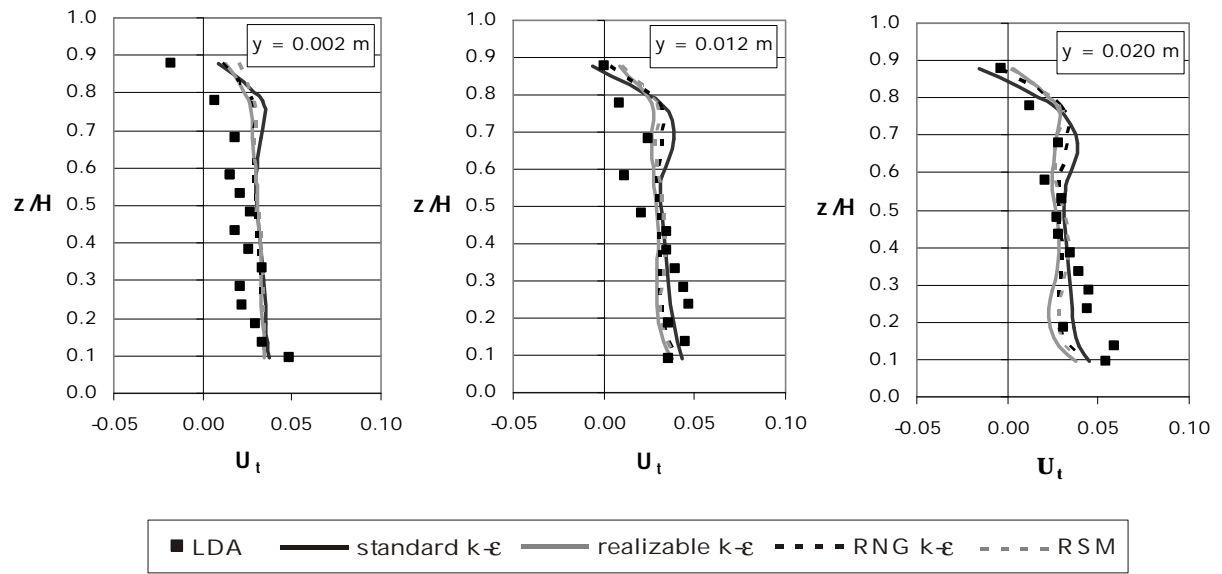


Fig. 3. The axial profiles of the tangential mean velocity at three distances from the tank wall, y .

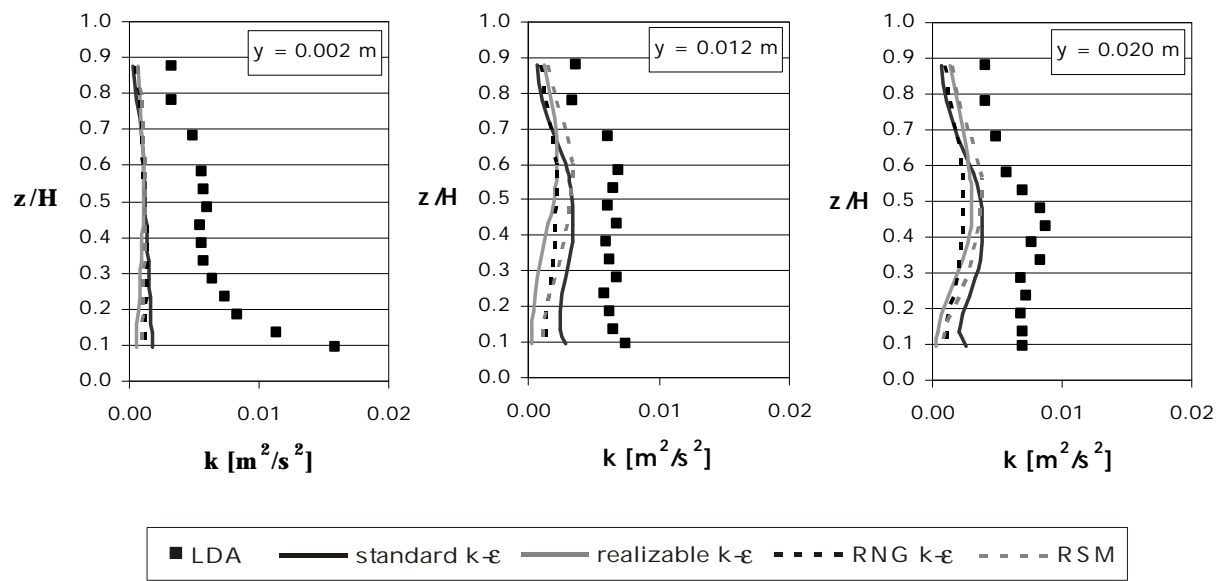


Fig. 4. The axial profiles of the kinetic turbulence energy at three distances from the tank wall, y .

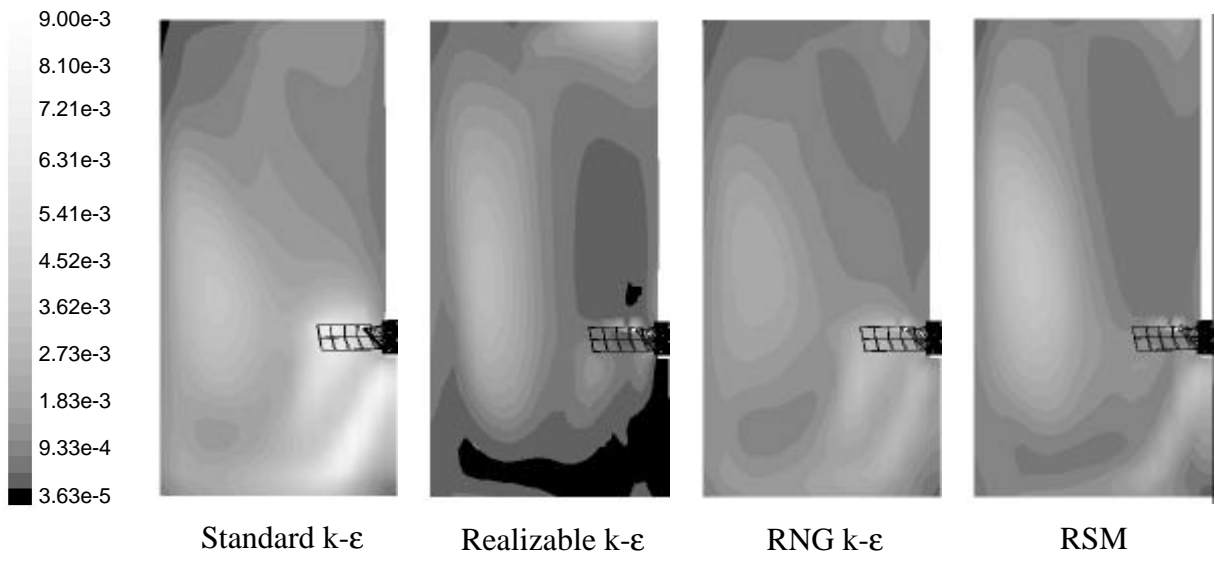


Fig. 5. Contours of the kinetic turbulence energy in the 45° plane between neighbouring baffles.